Military Technical College,
Kobry El-Kobbah,
Cairo, Egypt

9th International Conference
On Aerospace Sciences &
Aviation Technology

PENETRATION OF A SHAPED CHARGE JET INTO A METALLIC TARGET

By

Mohamed, S.Y.*, Riad, A.M.* and Kresha, Y.#

ABSTRACT

An analytical model has been developed to describe the jet penetration process into a metallic target. The model is essentially based on the modified Bernoulli's equation that incorporates the strengths of jet and target materials. The compression of jet length during its penetration through the target is considered in the analysis. The main equations predicting the jet length prior to impact and the governing equations describing the penetration process of a jet into a target are derived. These equations are arranged and compiled into a computer program. The input data to the program are easily determined.

The model is capable of predicting the time histories of jet penetration velocity, crater radius and depth of jet penetration into a target. In addition, the model predicts the total depth and time of jet penetration into a target. The results of the present model are compared with predicted and experimental results of other investigators; good agreement is obtained. Moreover, an experimental program has been conducted to assess the predictions of the model. Six shaped charges have been prepared and exploded at different distances from a steel target. For each shaped charge, the measured depth of penetration and crater radius at the target surface are compared with the corresponding model predictions; good agreement is obtained for the depth of penetration. However, a further analytical study is needed to improve the prediction of crater radius. Representative samples of the model predictions using the data of some tested shaped charges and the 105 mm shaped charge are presented and discussed.

KEY WORDS

Explosive cutting, Shaped charge, Terminal ballistics, Jet penetration, and Explosive welding.

* Egyptian Armed Forces.
# Assoc. Prof., Head of R. & D. Dept., Helwan Industrial Eng. Company, Cairo, Egypt.

1. INTRODUCTION

Analytical models capable of predicting the penetration of jets from shaped charges into a variety of target materials are extremely valuable to terminal ballistician. Many disciplines are involved, since shaped charges are used to penetrate or perforate metallic and non-metallic materials. Analytical models provide fast analytical predictions, where the time and resources available prohibit large hydrocode computer solutions.

Early analytical penetration models were based on Bernoulli principle. Both Birkhoff et al. [1] and Hill et al. [see Ref. [2]] developed a simple penetration theory from the hydrodynamic theory of impinging jets. Because of the hypervelocities of jets, they neglected the strengths and viscosities of jet and target materials, respectively. Moreover, they used the hydrodynamic assumption of incompressible, inviscid fluid flow. They considered a shaped charge jet of length L, density ρ_j and velocity V penetrating a semi-infinite, monolithic, target of density ρ_t. The penetration velocity is U, as shown in Fig. 1. They equated the pressure at jet-target interface and applied Bernoulli's equation so that:

$$\tfrac{1}{2}\,\rho_j\,(V-U)^2 = \tfrac{1}{2}\,\rho_t\,U^2. \qquad (1)$$

They derived the following equation that was used to calculate the total penetration Z:

$$Z = L\,(\rho_j / \rho_t)^{1/2}. \qquad (2)$$

The previous equation shows that the penetration is independent of the jet velocity. However, the eroding rate of jet and the final length of jet prior to impact depend on the jet velocity. There are several limitations to the simple theory; these are (i) it determines the primary penetration which corresponds to the depth of penetration when the jet vanishes, (ii) the effects of material strength, strain, strain rate and other properties on penetration are not considered, (iii) it doesn't predict the variation of penetration with standoffs, and (iv) it doesn't take into account the effects of jet velocity gradient and compressibility of jet on penetration.

Evans [see Ref. [2]] modified the simple theory by multiplying the density of jet by a factor; this factor was taken to be equal 1 when a continuous jet penetrated into a target and was equal two for the penetration of a particulated jet into a target. Pack and Evans [see Ref. [2]] noted the importance of target material strength on jet penetration. They proposed a semi-empirical factor added to the right hand side of Eqn. (2). For steel target, they determined that the effect of its strength reduced the jet penetration by as much as 30%. Moreover, they modified their equation by adding a term used for calculating the secondary penetration of a jet into a ductile target.

For a jet of variable velocity, such as that produces by a shaped charge, the jet length is not constant but increases with time. Therefore. Eqn. (2) is not applicable. Abrahamson and Goodier [see Ref. [3]] derived explicit formulae for the penetration of continuous, non-uniform velocity jets. They took the jet length as known at a given distance from the target but did not consider the relationship between jet length and distance from the charge; this made their results less useful for practical purposes.

Allison and Vitalli [see Ref. [3]] extended the theory of Abrahamson and Goodier to account for jet particulation. They assumed the following: (i) Existence of virtual origin; it was a point on the distance-time plan from which all jet particles originated, (ii) the strengths of jet and target materials were neglected and a minimum velocity, V_{min}, at which the penetration process of low velocity rear jet terminated was proposed, (iii) the compressibility effects of jet and target materials on penetration were neglected, (iv) the

entire jet was broken-up simultaneously, and (iv) each broken jet segment penetrated the target as a continuous jet. The principles proposed by Allison and Vitalli are still used today as the basis for penetration calculations.

DiPersio and Simon [see Ref. [2]] derived explicit formulae based on Allison and Vitalli's theory for three cases: (a) penetration before jet broke-up ($T<t_b$), (b) jet broke during penetration ($t_o < t_b \leq T$), and (c) jet broke before reaching the target ($t_b < t_o \leq T$); where T was the total time of penetration, t_b was the time of jet break-up, and t_o was the time when the tip reached the target. The predictions of these formulae were compared with experimental measurements; good agreement was obtained at short standoffs, up to three times the charge diameter. DiPersio et al. [see Ref. [3]] conducted an extensive experimental program to determine the reasons for the bad agreement at long standoffs. They concluded that the minimum jet velocity for penetration was not constant for a given jet or a target, but increased with standoffs.

Carleon et al. [see Ref. [4]], in an augmented version of the one-dimensional jet formation code, DESC, developed a theory for predicting the break-up of shaped charge jets and introduced an approximate method for determining the decrease in penetration with standoff. The break-up time of each portion of the jet was predicted or measured. Then, they applied their theory to predict the penetration of particulated jet considering the gap distance between jet particles and the depth of penetration as a continuous jet. Their theory gave a good agreement with experimental data.

In this paper, an analytical model has been developed to describe the penetration of a shaped charge jet into a metallic target. The present model is based on the modified Bernoulli's equation that incorporates the strengths of jet and target materials. Moreover, the compression in jet length during penetration is also considered in the analysis. The main equations determining the jet length prior to impact and the governing equations describing the penetration of a jet into a target are derived.

The model predictions are compared with analytical and experimental results of other investigators. An experimental program has been conducted to assess the model predictions. Six shaped charges are prepared and exploded at different distances from a steel target. The predicted depths of penetration and crater radii at the target surface are compared with experimental measurements. Moreover, representative samples of the model predictions using the data of some tested shaped charges and the 105 mm shaped charge are presented and discussed.

2. ANALYTICAL MODEL

To formulate the jet penetration into a semi-infinite metallic target, it is necessary to predict the jet length and its status, continuous or particulated, prior to its impact into a target. In the following, the analytical model includes: (i) modeling the break-up time of each jet element, (ii) modeling the initial length of formed jet, (iii) modeling the jet length just prior to its impact into a target, and (iv) modeling the jet penetration process into a target.

2.1. Modeling the Break-up Time of Each Jet Element

A typical shaped charge jet has a velocity gradient between its elements. This gradient causes the jet to elongate at sufficiently large standoffs. For continuous jet, the depth of penetration of a jet into a target is directly proportional to the jet length prior to impact. Once the jet particulates, the penetration decreases steadily and significantly. Therefore, the methods of delaying the onset of jet break-up are the major interest of the shaped

charge designers. Recently, many investigators studied the jet break-up phenomena, e.g. Hennequin [5], Chou and Carleone [see Ref. [5]], and Hirsch [6].

In the present model, the break-up time of each jet element, t_{b_i}, is determined using the semi-empirical formula developed by Hennequin [5]. The selection of this formula is based on its good predictive capability in comparison with the experimental measurements. The selected formula is:

$$t_{bi} = \frac{2 r_{ji}}{V_{pl}} \left[I_{FG} + (I_{FG} - 1) \frac{1}{\eta_O} \frac{V_{pl}}{2 r_{j_i}} \right], \tag{3}$$

where r_{ji} is the initial radius of each jet element, V_{pl} is the velocity difference between the jet particulated elements, I_{FG} is the shaped index factor, and η_o is the initial deformation rate of the jet. The factor I_{FG} defines the ratio between the volume of the imaginary cylinder surrounding the particulated element and the real volume of this element. It was found from experiments that the average value of shape index factor was equal to 1.46 and the velocity difference V_{pl} between the jet particulated elements was nearly constant [5]. The velocity difference is represented by:

$$V_{pl} = (V_{tip} - V_{tail}) / n_f, \tag{4}$$

where V_{tip} is the velocity of front element of jet, V_{tail} is the velocity of rear element of jet, and n_f is the number of elements resulted from the jet break-up. The value of this velocity difference was determined experimentally which varied from 80-140 m/s [5]. The initial radius of each jet element r_{ji} is determined by equating the volume of liner element with that of the corresponding jet element. The parameter η_o is equal to the ratio between the velocity difference between the particulated elements and the initial length of the particulated jet element. Substituting into Eqn. (3) for I_{FG} equals to 1.46 and η_o, the final equation of the break-up time for each jet element is:

$$t_{bi} = 2.92 \, (r_{ji} / V_{pl}) + 0.46 \, (L_i / V_{pl}), \tag{5}$$

where L_i is the length of the particulated jet element.

2.2. Modeling the Initial Length of Jet

The initial length of jet defines the jet length at the end of liner collapse process. The formed jet is assumed to be divided into n elements. For simplification, the elongation of each liner element from the moment of its collapse until the moment at which it arrives the cone axis is neglected as proposed by Hennequin [5] and Hirsch [6]. The elongation of each element is only considered after it arrives the cone axis. Modeling the initial length of jet consists of two main parts; these are: (a) modeling the initial jet length for the elements which have an inverse velocity gradient in between; the number of these elements is taken to be equal to (p-1) elements, and (b) modeling the initial jet length for the elements which have a velocity gradient in between; their number is taken to be equal to (n-p) elements. To calculate the initial length of jet, the velocity of each jet element after collapse process must be known.

The initial jet length of the (p-1) elements is represented by:

$$L_{j1} = \sum_{i=1}^{p-1} I_{1i} + \sum_{i=1}^{p-1} (V_1 - V_{i+1}) * \Delta t_i, \tag{6}$$

where l_{1i} is the length of each element of liner from the (p-1) elements, V_1 is the velocity of jet associated with the first element of collapsed liner, V_{i+1} is the jet velocity associated with the subsequent elements of collapsed liner, Δt_i is the difference between the arrival times of two successive elements to the cone axis.

The initial jet length of the (n-p) elements is represented by:

$$L_{j2} = \sum_{i=p}^{n} l_{2i} + \sum_{i=p}^{n} (V_{max} - V_{i+1}) * \Delta t_i \,, \tag{7}$$

where l_{2i} is the length of each element of liner from the (n-p) elements, V_{max} is the maximum velocity of jet, V_{i+1} is the jet velocity associated with the subsequent elements of collapsed liner.

Using Eqns. (6) and (7), the total initial length of jet is represented by:

$$L_{jt} = L_{j1} + L_{j2}. \tag{8}$$

2.3. Modeling the Length of Jet Prior to Impact into a Target

Once the initial jet length along the charge axis has been determined, the jet length prior to impact can also be determined considering the jet travel along the distance between the charge base and target surface, S. The velocity of each jet element is assumed to be constant during jet travel in air. The initial length of jet is compared with the liner projection along the cone axis, L cos α. If the initial jet length is less than L cos α, the distance S_D is (cf. Fig. 2):

$$S_D = S + \Delta L = S + (L \cos \alpha - L_{jt}). \tag{9}$$

The traveling time of the jet to cover the distance S, T_{bz}, is determined by:

$$T_{bz} = S_D / (V_{tip}). \tag{10}$$

If the time T_{bz} is less than break-up time of the front jet element, t_{b1}, the final length of jet prior to impact, L_{jf}, is determined by:

$$L_{jf} = L_{jt} + (V_{tip} - V_{tail}) * T_{bz}. \tag{11}$$

If the initial jet length is greater than L cos α, Eqns. (10) and (11) are used to calculate the final jet length prior to impact considering the distance S_D (= S- ΔL).

When the traveling time T_{bz} is greater than the break-up time t_{b1}, then the first element of jet has already particulated. The length of the break-up element is considered to be constant as proposed by Mayseless and Hirsch [7] and Titov [8]. Therefore, the length of jet prior to impact is determined by the sum of jet length until the moment at which its first element is broken-up and the stretching of jet length, excluding the length of the first element, during the time (T_{bz}- t_{b1}) after replacing the tip velocity of the jet by the velocity of the second element of jet.

If the traveling time T_{bz} is greater than the time of break-up of the second element t_{b2}, the length of jet prior to impact is calculated as the sum of the following: (i) length of jet until the first element has broken-up, (ii) the elongation of jet length, excluding the first element, during the time (t_{b2}- t_{b1}) considering the tip velocity of the jet is the velocity of the second element, and (iii) the stretching of jet length, excluding the second element, during the time

(T_{bz}- t_{b2}) after replacing the jet tip velocity by the velocity of the third element of jet. After each break-up of jet element, the break-up time of the next element is compared with the time T_{bz}, and the same concept is applied if t_{bi} is less than T_{bz}.

The cumulative length of jet defines the length of the formed jet until the moment at which the jet starts to break-up. The cumulative jet length, L_{jcum}, is determined by:

$$L_{jcum} = L_{jt} + (V_{tip} - V_{tail}) * t_{b1}, \tag{12}$$

2.4. Modeling Jet Penetration into a Target

Starting from the proposed formula of Eichelberger [see Ref. [3]], the interface pressure P_i is represented by:

$$P_i = \lambda \rho_j (V_i - U_i)^2 = \rho_t U_i^2 + 2\sigma, \tag{13}$$

and

$$\sigma = \sigma_t - \sigma_j, \tag{13)a}$$

where λ is a constant which is equal to one for a continuous jet and less than one for a particulated jet [see Ref. [3]], ρ_j is the density of jet material, V_i is the velocity of jet penetrating element, U_i is the penetration velocity, ρ_t is the density of target material, σ_t is the resistance factor for target material, and σ_j is the resistance for jet material. Each resistance factor is taken as 1/3 the value of the static uniaxial yield strength of material.

Using Eqn. (13), the penetration velocity for each penetrating jet element is represented by:

$$U_i = \frac{V_i - \sqrt{\varphi V_i^2 + A_t(1-\varphi)}}{(1-\varphi)}, \tag{14}$$

where

$$\varphi = \frac{\rho_t}{\lambda \rho_j} \quad \text{and } A_t = \frac{2\sigma}{\lambda \rho_j}. \tag{14)a}$$

The rate of decreasing of length of jet penetrating element, L_{jfi}, is:

$$\frac{dL_{jfi}}{dt} = -(V_i - U_i). \tag{15}$$

The rate of change of penetration depth for each penetrating element, Z_i, is:

$$\frac{dZ_i}{dt} = U_i. \tag{16}$$

For each incremental time Δt, the penetration velocity U_i, the depth of penetration Z_i and the eroded length of the penetrating element of jet are determined using Eqns. (14), (15) and (16). Due to the velocity gradient between jet elements, the remaining jet length is assumed to be compressed during the penetration of the interacting element of jet with the target; this decrease is represented by:

$$L_C = ((V_i - U_i) - V_{tail}) * \Delta t, \tag{17}$$

where L_C is the decrease in jet length due to its compression, V_i is the velocity of penetrating element of jet, U_i is the penetration velocity, and V_{tail} is the velocity of rear element of jet.

For the next time step, the jet velocity of the penetrating element represents the current jet tip velocity V_i. The same procedures for calculating the parameters associated with the penetration of jet element during the first time step are followed. The penetration process terminates if: (i) the remaining jet is not capable of exerting the required force for moving the target material away from the jet path; this is corresponding to the so-called "cut-off velocity" which is equal to about 1000 m/s [9], or (ii) the jet length is totally consumed. The total depth of penetration is represented by the sum of penetration of the individual elements of jet.

For a particulated jet, the depth of penetration into a target, Z', is calculated using a formula developed by Carleone et. al. [see Ref. [4]]:

$$Z' = Z\left(1 - \frac{g}{g_o}\right), \tag{18}$$

where Z is the total depth of penetration of continuous jet, g is the sum of gap distances between the break-up jet elements ($= \Sigma\, g_i$), g_o is an empirical constant, which is equal to 6.5 for precision shaped charges and 4.6 for small charges. For each break-up jet element, the gap distance g_i is calculated using the following equation:

$$g_i = (V_i - V_{i+1}) * (T_{bZ} - t_{bi}). \tag{19}$$

To calculate the jet penetration depth, the traveling time of the formed jet in air is calculated and the status of jet at the moment of its impact into a target is determined. If the jet reaches the target after being broken-up, its total penetration is first predicted using the same procedures for continuous jet, then the final depth of penetration is predicted using Eqn. (18).

To model the crater radius, Eqn. (13) is used considering the radial velocity U_c is equal to the penetration velocity of the penetrating jet element U_i [10]. Moreover, the acting pressure on target material changes with crater radius so that:

$$P_r = \frac{a_o . p_i}{a}, \tag{20}$$

where a_o is the cross-sectional area of penetrating jet element, p_i is the corresponding acting pressure, a is the formed crater area, and P_r is the corresponding pressure. The pressure p_i is represented by: (cf. Eqn. (13)):

$$p_i = \frac{\lambda}{2}\rho_j (V_i - U_i)^2 + \sigma_j, \tag{21}$$

where V_i is the velocity of the penetrating jet element and U_i is its penetration velocity represented by Eqn. (14). Equating U_C by $\frac{dr_C}{dt_C}$ and substituting Eqn. (20) into the right hand side of Eqn. (13) yields:

$$U_C = \frac{dr_C}{dt_C} = \left(\frac{2p_j a_o}{\rho_t a} - \frac{2\sigma_t}{\rho_t} \right)^{0.5} \quad (22)$$

The ratio $\frac{a_o}{a}$ can be written as $\left[\frac{r_{ji}}{r_C}\right]^2$, the square of the ratio of radius of jet penetrating element to crater radius. Equation (22) is rewritten in simplified form as:

$$dt_C = \frac{dr_C}{\sqrt{\frac{A}{r_C^2} - B}}, \quad (23)$$

where

$$A = \frac{2r_{ji}^2 p_j}{\rho_t}, B = 2\frac{\sigma_t}{\rho_t} \quad (23)a$$

Integrating Eqn. (23), the final expression for the crater radius as a function of time t_c is:

$$r_C = \sqrt{\frac{A}{B} - \left(\sqrt{\frac{A}{B} - r_{ji}^2} - t_C \sqrt{B} \right)^2} \quad (24)$$

The radius of the penetrating jet element r_{ji} is determined using the following equation:

$$r_{ji} = \sqrt{\frac{m_{ji}}{\pi L_{ji} \rho_j}}, \quad (25)$$

where m_{ji} is the mass of penetrating jet element, and L_{ji} is the length of the penetrating element of jet.

A compete formulation of the analytical model that describes the penetration process of a shaped charge jet into a metallic target has been introduced. The governing equations of the present model are arranged and compiled into a computer program. The input data to the program are easily determined.

3. EXPERIMENTAL WORK

The main objective of experimental work was to assess the predictions of the present model. The experimental facilities of the shaped charge laboratory, Explosives Dept., MTC, were used to prepare six small size shaped charges with different high explosives and liner materials. Each prepared charge was designated by letters and number (e.g. charge no. 1 is designated by Ch1). Figure 3 shows a schematic drawing of a prepared shaped charge. The data of each prepared shaped charge are listed in Table 1. The interested reader could be referred to the original reference for further details [11].

The target material is selected to be steel. The characterization of the steel target had been performed in the Dept. of Research and Development, Helwan Engineering Industrial

Table 1. Data of prepared shaped charges and the 105 mm [11].

Charge Design.	Base Dia., R_B [mm]	Cone Angle, 2α [°]	Cone Mat.	Liner Density, ρ_L [g/cm^3]	Liner Thick., T_L [mm]	Expl. Type	Expl. Density, ρ_{exp} [g/cm^3]	Dist., S [mm]
Ch1	14.9	60	Al.	2.6	0.8	RDX	1.77	15
Ch2	14.9	60	Cu	8.9	0.8	HMX	1.89	15
Ch3	14.9	60	Cu	8.9	0.8	TNT	1.54	15
Ch4	14.9	60	Cu	8.9	0.8	RDX	1.77	15
Ch5	14.9	60	Cu	8.9	0.8	RDX	1.77	30
Ch6	14.9	60	Cu	8.9	0.8	RDX	1.77	45
105 mm	87	42	Cu	8.9	3.0	Comp.B	1.72	250

Company (Formerly MF No. 99), Helwan, Cairo. The target characterization includes: (i) chemical analysis, (ii) measurement of hardness and using conversion tables to determine the target strength. The chemical composition of the ingredients of target material was determined using a Direct Emission Spectrometer Analyzer named Polyvac-E982; two specimens were used to perform this test. In addition, three specimens were prepared and the hardness was measured using a Rockwell Hardness Tester, Model Indentec. The hardness was measured at different points on each specimen surface.

The ballistic tests of the prepared shaped charges were carried out in the shaped charge laboratory, Explosives Dept., MTC. The ballistic set-up consists mainly of: (i) detonation chamber, (ii) fire control device, and (iii) prepared shaped charge, and (iv) steel target plates. A photograph of the ballistic set-up is shown in Fig. 4. For each tested shaped charge, the ballistic measurements were mainly concerned with the determination of the depth of jet penetration into a steel target and the crater radius at the target surface. The ballistic measurements were carried out in Helwan Engineering Industrial Company. The penetrating steel plates were cut using EDM wire cutting technique. For each tested shaped charge, X-ray technique was used to determine the aforementioned ballistic measurements.

4. RESULTS AND DISCUSSIONS

The present model is capable of predicting the time histories of penetration velocity U_t, depth of penetration Z_t, and the crater radius r_c. Moreover, the present model determines the total length of jet prior to impact, the total depth of jet penetration into a target and the total time of penetration. In the following, the present results are divided into: (i) model validation, (ii) results of target material characterization, (iii) comparison of current experimental results with model predictions, and (iv) model predictions.

4.1. Model Validation

Chanteret [12] predicted the change of break-up time of jet with jet velocity for the 100 mm conical shaped charge. He fed his model with the following data of a shaped charge: a cone angle of 60°, and a copper liner wall thickness of 2 mm. The explosive charge was consisted of a mixture of hexogen and TNT with equal percent. Moreover, He fed his model with the value of velocity difference, V_{pl}; this difference was taken to be equal to 115 m/s. The data used by Chanteret are fed into the present model and the predicted change

of break-up time with jet velocity is plotted in Fig. 5. The corresponding predicted change of break-up time with jet velocity obtained by Chanteret is also plotted on the same figure. Good agreement is generally obtained between the predicted break-up time of the present model and that predicted by Chanteret.

Chanteret [12] determined experimentally the change of jet velocity with jet cumulative length for the 100-mm conical shaped charge. Figure 6 plots the predicted change of jet velocity with jet cumulative length; the corresponding experimental measurements obtained by Chanteret [12] are depicted on the same figure. Good agreement is obtained between the predictions of the present model and experimental measurements of Chanteret except for the region of the rear of jet where the measured jet velocities by Chanteret are higher than those predicted by the model. This difference may be attributed to the effect of the wave shaper that is not considered in the model. The wave shaper provides a better benefit of the explosive energy by directing the detonation wave nearly perpendicular to the liner wall. This effect appears strongly at the liner base where the amount of explosive is relatively small.

4.2. Results of Target Material Characterization

The chemical composition of the ingredients of the steel target is listed in Table 2. Moreover, the mean of the measured values of target hardness is 41.5 Rc. The corresponding tensile strength determined from the conversion tables is 1400 MPa.

4.3. Comparison of Experimental Results with Model Predictions

The prepared charges during the experimental work are exploded at different distances from a steel target. For each shaped charge, both the jet penetration depth and the carter entrance radius are measured. Table 3 lists the experimental measurements due to explosion of the prepared charges and the corresponding predicted results of the present model. In addition, Fig. 7 shows X-ray photographs for the penetration depths of the Ch1, Ch2, and Ch3 charges into a steel target, respectively.

The predicted values of penetration depth are compared with the corresponding experimental measurements; good agreement is generally obtained. Moreover, it is found that the maximum error is 17.4% for the charge Ch4. The obtained errors between predicted and experimental results can be attributed to the following: (i) the neglect of the charge height behind the cone apex angle, (ii) the neglect of the effect of charge confinement, and (iii) the after flow residual jet penetration. The suggested reasons for errors are difficult to be represented in the present analytical model.

The predicted results of crater radii are far from the corresponding experimental measurements. An additional analytical investigation is needed to suit a better agreement between the model predictions and experimental measurements. The trend of the current predicted results is similar to that obtained by Held [10] who concluded that: (i) the predicted crater radii are generally greater than the corresponding measured ones, and (ii) an extensively analytical study is needed to develop a formula capable of predicting a crater radius close to experimental measurement.

4.4. Model Predictions

In the following, representative samples of the current predicted results using the charges Ch1, Ch2, and/or the 105 mm, respectively, are presented. The input data to the model are listed in Table 1. Figure 8 shows the predicted change of jet break-up time with jet velocity for Ch1 and Ch2, respectively. The figure shows that the break-up time of jet element

Table 2. Chemical composition of steel target in percent.

Element	Fe	C	Si	Mn	Ni	Al	Cu	Cr	Mo	Others
Percent	96.2	0.12	1.57	1.29	0.066	0.044	0.093	0.19	0.18	0.247

Table 3. Predicted and measured depth of penetration and crater radius for each used charge.

Charge Designa.	Penetration depth [mm]		Crater entrance radius [mm]	
	Predicted	Measured	Predicted	Measured
Ch1	16	19	14	5
Ch2	22	26	8.8	4
Ch3	16	19	6	3
Ch4	19	23	6	3.7
Ch5	35	34	4.2	3.5
Ch6	46	42	3.6	3

decreases with the increase in its velocity. This may be attributed to the direct relation between the stretching of jet element and its velocity. For jet elements of high velocity, faster stretching in the jet length occurs which accelerates the elements to be broken-up. The model is capable of predicting the break-up time of each jet element. For the shaped charge Ch1, the break-up time of the front jet element, which has a velocity of 6504 m/s, is 39 μs whereas, the break-up time of the rear element of jet, which has a velocity of 1154 m/s, is 97 μs. For the shaped charge Ch2, The break-up time of the front element of jet is 33 μs whereas, the break-up time of rear element of jet is 106 μs.

Figure 9 plots the predict change of jet velocity with jet cumulative length for Ch1, Ch2 and the 105 mm shaped charges, respectively. The cut-off velocity fed into the model is considered to be equal to 1000 m/s [9]. For each shaped charge, it is clear from figure that the jet cumulative length produced from the collapsed liner increases with the increase of velocity gradients. The present model is capable of predicting the current cumulative length of jet originated during the collapse process of liner elements and the total cumulative length of jet.

Figure 10a plots the time histories of jet penetration depth for the charges Ch1 and Ch2, respectively, whereas Fig. 10b plots the corresponding time history for the 105 mm shaped charge. With the increase in penetration time, the penetration depth increases due to the sum of the incremental depths achieved by the successive jet elements. For Ch1 and Ch2, the total depth of penetration is reached when the penetrating jet element having the cut-off velocity starts to penetrate the target whereas, the penetration ceases for the 105 mm charge when the jet is completely consumed. The present model predicts the total depths and times of penetration for the charges Ch1, Ch2, and the 105 mm, respectively. The predicted penetration depths are 16, 22, and 250 mm whereas the corresponding total penetration times are 8, 13, and 135 μs, respectively.

The time histories of jet penetration velocity for the charges Ch1 and Ch2, respectively, are plotted in Fig. 11a whereas; the corresponding time history for the 105 mm is plotted in Fig. 11b. The current penetration velocity is a function of jet velocity of penetrating element; the velocity of jet elements varies from the maximum value at the tip element to the minimum value at its rear element. When penetration starts, the penetration velocity

has its maximum value. Then the velocity decreases with the increase of penetration time until it reaches its minimum value, which is corresponding to the considered cut-off velocity of jet [9]; the jet penetration is assumed to be stopped at such penetration velocity. The predicted maximum penetration velocities for the charges Ch1, Ch2, and the 105 mm are 3356, 2536 and 3020 m/s, respectively.

Finally, the predicted time histories of crater entrance radius for Ch1 and Ch2, respectively, are plotted in Fig. 12a whereas; the corresponding time history for the 105 mm is plotted in Fig. 12b. Initially, the crater radius is equal to the radius of front element of jet then, it increases with the time until it reaches its final value. The crater expansion time is different from the penetration time. Radial crater expansion as a function of time increases remarkably as the penetration velocity of front jet element increases. The predicted values of jet tip radii for Ch1, Ch2, and the 105 mm charges, respectively, are 2, 3, and 7 mm and the corresponding crater entrance radii are 14, 8, and 23 mm.

5. CONCLUSIONS

An analytical model has been developed to describe the jet penetration process into a metallic target. The present model includes the effects of strengths of jet and target materials and the compression of jet length during its penetration on jet performance. The main equations predicting the initial length of jet, the jet length prior to impact and the main parameters associated with the jet penetration process into a target are derived. These equations are compiled into a computer program; the input data to the program are easily determined. The model predictions are compared with the predicted and experimental results of other investigators; good agreement is obtained.

Six shaped charges of different explosives and liner materials are prepared and exploded at different distance from a steel target. For each shaped charge, both the depth of penetration and crater radius at the target surface are measured and compared with the corresponding analytical results. Good agreement is obtained between the predicted and measured depth of penetration. However, a further analytical study is still needed to suit the measured crater radii with that of the model predictions. In addition, representative samples of the model predictions using the data of shaped charges, designated by Ch1 and Ch2, and the 105 mm charge are presented and discussed. The present model has a good predictive capability and can be extended to describe the jet penetration formed from different liner geometries into a metallic target.

6. REFERENCES

1. G. Birkhoff, G., MacDpougal, D. P., Pugh, E. M. and Taylor, G.,"Explosives with Lined Cavities", J. Appl. Phys., Vol. 19, pp. 563-582 (1948).
2. Walters, W., Flis, W. S. and Chou, P. C., "A Survey of Shaped-Charge Jet Penetration Models", Int. J. Impact Engng., Vol. 7, No 3, pp. 307-325 (1988).
3. Walters, P. and Zukas, J. A., "Fundamentals of Shaped Charges", Wiley Interscience Publication, John Wiley and Sons, New York, U.S.A. (1989).
4. Battacharya, R., Singh, S., Kishore, P., Raychaudhuri, T. K. and Sharma, V. K. "A Simplified Approach for Development of One-Dimensional Time Dependent PC Based Code for Shaped Charge Design", 16th Int. Symp. On Ballistics, San Francisco, CA, USA, September 1996.
5. Hennequin, E. "Modeling of Shaped Charge Jet Break-up", Propellants, Explosives, Pyrotechnics Vol. 21, pp. 181-185 (1996).

6. Hirsch E.,"A Formula for the Shaped Charge Jet Break-up Time", Propellants, Explosives, Pyrotechnics, Vol. 4, pp. 89-94 (1979).
7. Maysless, M. and Hirsch, E.,"The Penetration-Standoff Relation of Jets with Non-Linear Velocity Distribution", 18th Int. Symp. On Ballistics, San Antonio, 15-19 November 1999.
8. Titov, V., "Ultimate Elongation of Metallic Shaped-Charge Jets", 16th Int. Symp. On Ballistics, San Francisco, September 1996.
9. Chemin, C., Qingming, T., Juxian, G., Dongying, Y. and Yuyan, W.,"A Theory on the Reduction of Penetration Power of Metal Jets in Certain Composites", Symp. of Intense Dynamic Loading and its Effects, China, 3-7 June 1986.
10. Held, M.,"Verification of the Equation for Radial Crater Growth by Shaped Charge Jet Penetration", Int. J. Impact Engng., Vol. 17, pp. 387-398 (1995).
11. Mohamed, S. Y.,"Factors Affecting the Shaped Charge Performance", M. Sc. Thesis, M.T.C., Cairo, Egypt (2000).
12. Chanteret, P.Y.,"Considerations about the Analytical Modeling of Shaped Charges", Propellants, Explosives, Pyrotechnics, Vol. 18, pp. 337-344 (1993).

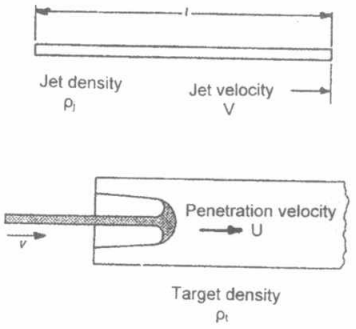

Fig. 1. Jet penetration into a target [2].

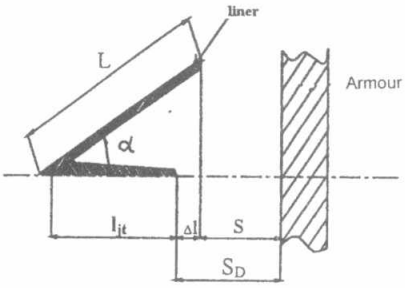

Fig. 2. A schematic drawing for a jet traveling along the charge axis.

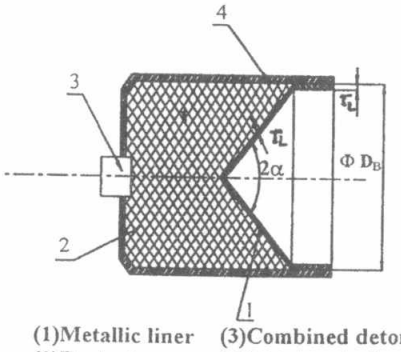

(1)Metallic liner (3)Combined detonator
(2)Explosive (4)Metallic casing

Fig. 3. A diagrammatic scheme of a prepared shaped charge.

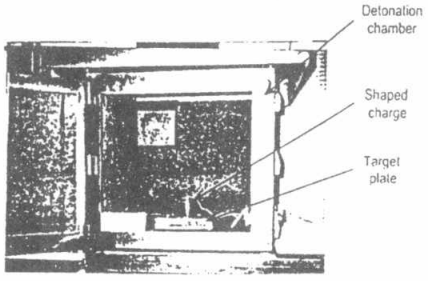

Fig. 4. A photograph of ballistic set-up.

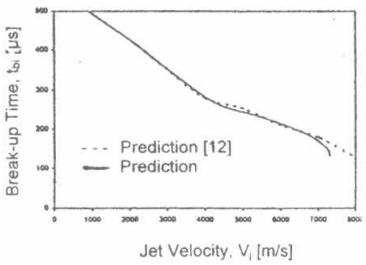

Fig. 5. The predicted change of jet break-up time with jet velocity for the 100 mm shaped charge, analytical results obtained by Chanteret [12].

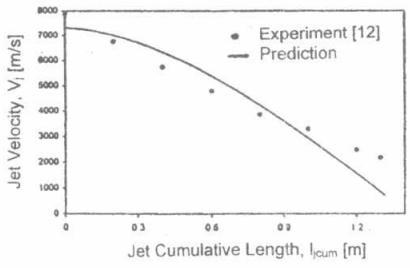

Fig. 6. The predicted change of jet break-up time with jet cumulative length for the 100 mm shaped charge, experimental results obtained by Chanteret [12].

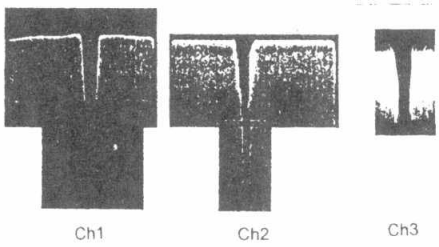

Fig. 7. X-ray photographs of the crater profiles produced by explosion of the charges Ch1, Ch2 and Ch3, respectively.

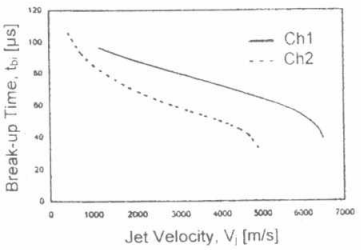

Fig. 8. The predicted change of jet break-up time with jet velocity for the charges Ch1 and Ch2, respectively.

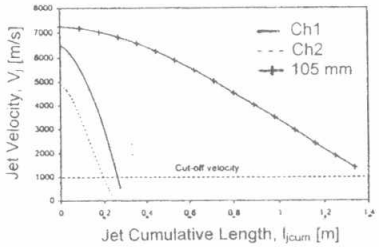

Fig. 9. The predicted change of jet break-up time with jet cumulative length for the charges Ch1, Ch2, and 105 mm, respectively.

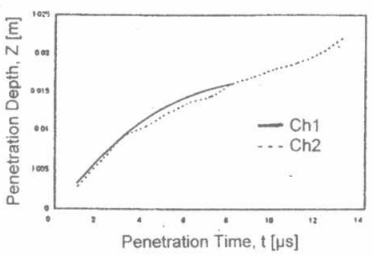

Fig. 10a. The time histories of predicted penetration depth for the charges Ch1, and Ch2, respectively.

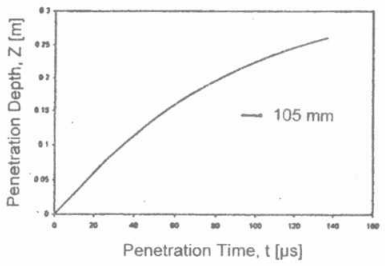

Fig. 10b. The time history of predicted penetration depth for the 105 mm shaped charge.

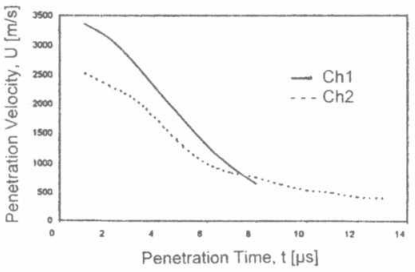

Fig. 11a. The time histories of predicted penetration velocity for the charges Ch1, and Ch2, respectively.

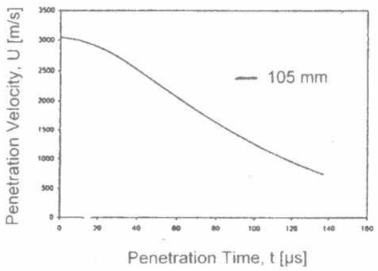

Fig. 11b. The time history of predicted penetration velocity for the 105 mm shaped charge.

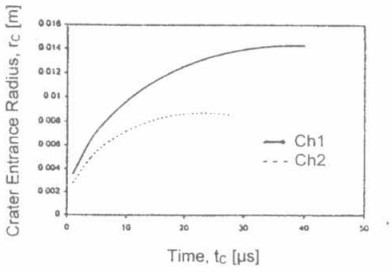

Fig. 12a. The predicted change of crater radius with time for the charges Ch1 and Ch2, respectively.

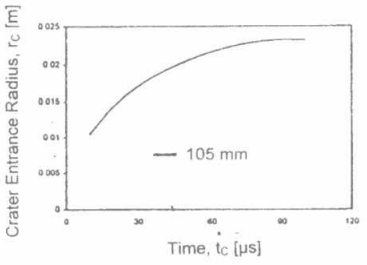

Fig. 12b. The predicted change of crater radius with time for the 105 mm charge.